Supporting Information

Active Site of Catalytic Ethene Epoxidation: Machine-Learning Global Pathway Sampling Rules Out the Metal Sites

Dongxiao Chen, Pei-Lin Kang and Zhi-Pan Liu*

Email: zpliu@fudan.edu.cn

Collaborative Innovation Center of Chemistry for Energy Material, Shanghai Key Laboratory of Molecular Catalysis and Innovative Materials, Key Laboratory of Computational Physical Science, Department of Chemistry, Fudan University, Shanghai 200433, China

Table of Contents

1. SSW-NN methodology and G-NN potential construction

1.1 Architecture of neural network potential

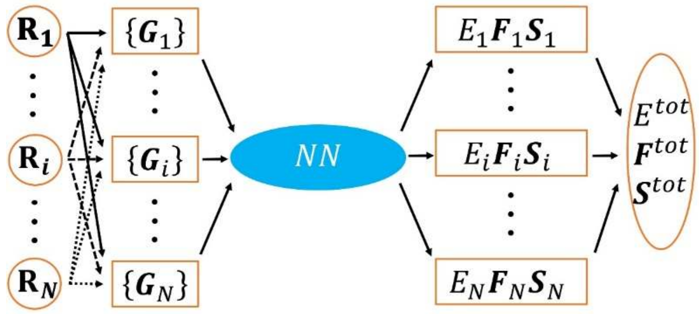

Scheme S1. Scheme of the HDNN architecture. The subscripts (1, *i*,…, *N*) are atom indices and represent the total atoms in a structure. The inputs of NN are a set of structural descriptors {***G***}, which are constructed from the Cartesian coordinates {**R**} of the structure, while the outputs of NN are the atomic properties { E_i, $\boldsymbol{F}_i$, $\boldsymbol{S}_i$ }, i.e., energies, forces, and stresses. The overall properties, E^{tot}, $\boldsymbol{F}^{tot}$, and $\boldsymbol{S}^{tot}$, can be calculated from the individual atomic contributions.

In this work, we utilized the high dimensional neural network (HDNN) scheme to construct the global NN (G-NN) potential, as shown in **Scheme S1**. The input nodes to NN are a set of structural descriptors of a structure, as discussed in our previous works.[1-3] The total energy E^{tot} of the structure can be composed as a linear combination of its atomic energy E^i from the output of NN

$$E^{tot} = \sum_i E_i \qquad (1)$$

Consistently, the atomic force can be analytically derived from the total energy, i.e., the force component $F_{k,\alpha}$ ($\alpha = x$, y, or z) acting on atom k is the derivative of the total energy E^{tot} with respect to coordinate $\mathrm{R}_{k,\alpha}$. In combination with Eq. 1, the force component $F_{k,\alpha}$ then is related to the derivatives of the atomic energy E^i with respect to the j^{th} structural descriptors of atom i, $G_{j,i}$

$$F_{k,\alpha} = -\frac{\partial E^{tot}}{\partial \mathrm{R}_{k,\alpha}} = -\sum_{i,j} \frac{\partial E_i}{\partial G_{j,i}} \frac{\partial G_{j,i}}{\partial \mathrm{R}_{k,\alpha}} \qquad (2)$$

Similarly, the element $\sigma_{\alpha\beta}$ of static stress tensor matrix can be analytically derived as

$$\sigma_{\alpha\beta} = -\frac{1}{V} \sum_{i,j,d} \frac{(\boldsymbol{r}_d)_\alpha (\boldsymbol{r}_d)_\beta}{r_d} \frac{\partial E_i}{\partial G_{j,i}} \frac{\partial G_{j,i}}{\partial r_d} \qquad (3)$$

where $\boldsymbol{r}_d$ and r_d are the distance vector, constituted by $G_{j,i}$ and its module, respectively, and V is the volume of the structure.

1.2 Dataset generation and training of global NN potential

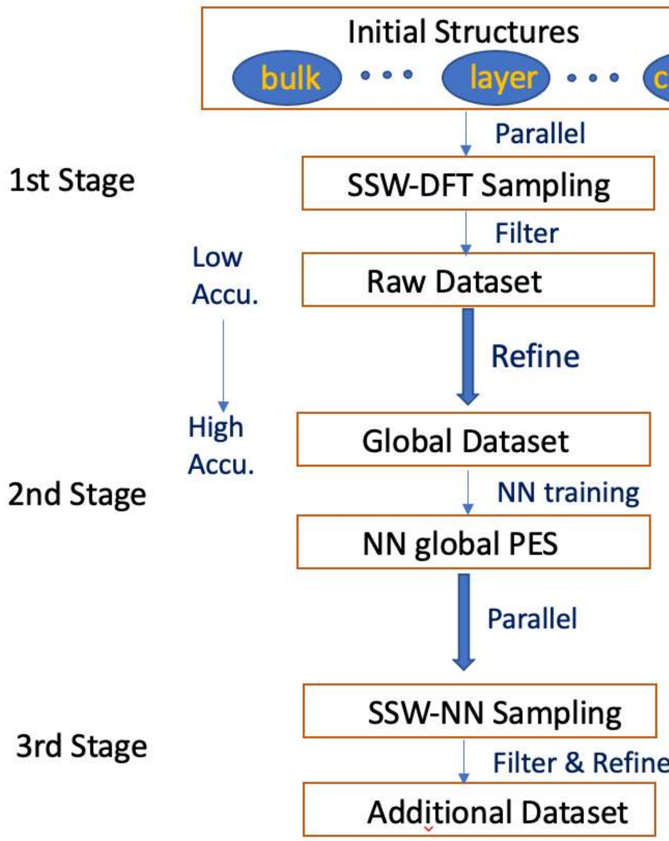

Scheme S2. Procedure for the generation of the global training dataset by SSW global optimization. In the first stage, the SSW sampling is typically performed by low accuracy DFT calculations. In the second stage, the global dataset is first refined with high accuracy DFT setups, and then a NN training is performed based on the accurate global dataset. In the third stage, an additional dataset is generated by SSW sampling utilizing the previously obtained NN PES, and is fed into the global dataset. A new cycle of NN training then starts based on the new global dataset (back to stage 2).

Undoubtedly, the quality of the potential energy surface (PES) of G-NN is largely determined by its training dataset. Here we utilized the stochastic surface walking (SSW) global optimzation[4-6] to generate a global dataset, which is fully automated and does not need a priori knowledge on the system, such as the structural motif, e.g. bonding patterns and symmetry. The final obtained Ag-C-H-O global dataset contains a variety of structural patterns on the global PES, as summarized in **Table S1**. In brief, the SSW-NN method involves three stages to generate the global dataset (see **Scheme S2**), as described below.

(i) **The first stage** generates a raw dataset, which contains the most common atomic environment and serves to build an initial NN PES. This is done by performing density functional theory (DFT) SSW global optimization in a massively parallel way. In this stage, the DFT calculations have low accuracy set-ups and small unit cells to speed up the SSW search. By collecting and screening the structures from SSW trajectories, a raw dataset is obtained.

(ii) **The second stage** trains a NN global PES. This is done by refining the dataset using DFT calculations with high accuracy setups, followed by NN training on the accurate global dataset. The NN architecture applied in this stage utilizes a small set of structural descriptors and a small network size.

(iii) **The third stage** iteratively expands the global dataset. It targets to increase the predictive power of NN PES by incorporating more structural patterns into the dataset. This is done by performing SSW PES search using the NN PES obtained in the second stage, starting from a variety of initial structures. These initial structures are randomly constructed, and also include large systems with many atoms per unit cell. The structures from all the SSW trajectories are collected and filtered to generate an additional dataset. The new dataset is then fed to the global dataset to start a new cycle of NN training (back to stage 2).

Table S1. Structure information of the global dataset for NN training. Listed data are the number of the structures in the global dataset, as distinguished by the chemical formula, the number of atoms (Natoms), the type of structures (cluster, bulk, layer) and its total number (Ntotal).

Chemical Formula	Natoms	Ncluster	Nlayer	Nbulk	Ntotal
Ag14	14	0	3	30	33
Ag15	15	85	5	726	816
Ag16	16	0	1	6554	6555
Ag17	17	0	0	19	19
Ag28	28	0	0	34	34
Ag29	29	0	15	0	15
Ag30	30	0	31	32	63
Ag31	31	0	0	74	74
Ag32	32	0	2	93	95
Ag64	64	0	94	0	94
O1-Ag16	17	0	7	32	39
O1-Ag18	19	23	0	0	23
O1-Ag20	21	0	1	11	12
O1-Ag21	22	0	1	0	1
O1-Ag24	25	0	0	62	62
O2-Ag16	18	0	6	53	59
O2-Ag19	21	0	2	0	2
O2-Ag20	22	0	2	9	11
O2-Ag78	80	0	43	0	43
O3-Ag16	19	0	3	39	42
O3-Ag20	23	0	2	11	13
O3-Ag33	36	0	53	30	83

O3-Ag37	40	0	49	0	49
O4	4	0	15	0	15
O4-Ag16	20	0	6	54	60
O4-Ag24	28	0	0	32	32
O4-Ag76	80	0	48	0	48
O5-Ag8	13	0	1	64	65
O5-Ag35	40	0	31	0	31
O5-Ag76	81	0	12	0	12
O6-Ag4	10	0	0	2942	2942
O6-Ag8	14	0	0	23	23
O6-Ag16	22	0	1	78	79
O6-Ag30	36	0	47	97	144
O6-Ag34	40	0	101	0	101
O6-Ag68	74	0	33	0	33
O6-Ag72	78	0	60	0	60
O6-Ag75	81	0	5	0	5
O6-Ag76	82	0	9	0	9
O7-Ag8	15	0	0	1283	1283
O8-Ag6	14	97	0	0	97
O8-Ag8	16	105	5	3594	3704
O8-Ag16	24	0	18	99	117
O8-Ag24	32	66	0	82	148
O8-Ag28	36	0	73	9	82
O8-Ag70	78	0	28	0	28
O8-Ag72	80	0	26	0	26
O9-Ag8	17	0	0	46	46
O10-Ag8	18	0	5	288	293
O10-Ag16	26	0	1	43	44
O10-Ag24	34	0	0	29	29
O10-Ag72	82	0	10	0	10
O11	11	0	78	24	102
O11-Ag16	27	0	0	13	13
O11-Ag25	36	0	57	82	139
O11-Ag69	80	0	31	0	31
O11-Ag71	82	0	108	0	108
O11-Ag72	83	0	21	0	21
O12-Ag8	20	36	8	1171	1215
O12-Ag16	28	0	3	50	53
O12-Ag24	36	24	0	60	84
O12-Ag72	84	0	163	0	163
O12-Ag85	97	0	77	0	77
O12-Ag88	100	0	35	0	35
O14-Ag16	30	0	1	44	45
O15-Ag16	31	0	1	48	49
O15-Ag21	36	0	130	181	311
O15-Ag77	92	0	1	0	1
O16-Ag12	28	0	0	211	211
O16-Ag16	32	0	19	26	45
O16-Ag32	48	0	8	58	66
O18-Ag18	36	0	53	93	146
O18-Ag97	115	0	50	0	50
O20-Ag16	36	0	65	96	161
O22-Ag16	38	0	0	205	205
O24-Ag16	40	0	0	14	14
O35-Ag210	245	0	2	0	2

O36-Ag210	246	0	1	0	1
H1-Ag16	17	0	9	16	25
H1-O3-Ag32	36	0	48	0	48
H1-O5-Ag34	40	0	35	0	35
H1-O6-Ag29	36	0	45	46	91
H1-O8-Ag27	36	0	43	0	43
H1-O11-Ag24	36	0	35	37	72
H1-O13-Ag65	79	0	26	0	26
H1-O15-Ag20	36	0	73	98	171
H1-O18-Ag17	36	0	43	60	103
H1-O20-Ag15	36	0	45	41	86
H2-Ag16	18	0	3	240	243
H2-O1-Ag27	30	0	83	0	83
H2-O3-Ag31	36	0	64	0	64
H2-O6-Ag28	36	0	53	63	116
H2-O8-Ag26	36	0	53	0	53
H2-O11-Ag23	36	0	64	59	123
H2-O15-Ag19	36	0	122	102	224
H2-O18-Ag16	36	0	63	63	126
H2-O20-Ag14	36	0	57	52	109
H2-C1-O2-Ag16	21	0	63	1	64
H2-C1-O2-Ag27	32	0	81	1	82
H2-C2-O3-Ag27	34	0	185	12	197
H3-Ag16	19	0	74	174	248
H3-O3-Ag30	36	0	9	0	9
H3-O3-Ag34	40	0	26	0	26
H3-O6-Ag27	36	0	9	10	19
H3-O8-Ag25	36	0	9	0	9
H3-O11-Ag22	36	0	13	11	24
H3-O15-Ag18	36	0	16	16	32
H3-O18-Ag15	36	0	9	7	16
H3-O20-Ag13	36	0	12	8	20
H3-C1-O2-Ag18	24	0	49	1	50
H3-C2-O2-Ag32	39	0	2	0	2
H3-C2-O3-Ag23	31	0	2	0	2
H3-C2-O3-Ag24	32	0	35	0	35
H3-C2-O3-Ag27	35	0	18	0	18
H4-Ag12	16	1	0	0	1
H4-O3-Ag29	36	0	12	0	12
H4-O6-Ag26	36	0	16	10	26
H4-O8-Ag24	36	0	9	0	9
H4-O11-Ag21	36	0	13	12	25
H4-O15-Ag17	36	0	21	22	43
H4-O18-Ag14	36	0	12	10	22
H4-O20-Ag12	36	0	12	8	20
H4-C1-O2-Ag36	43	0	535	0	535
H4-C1-O3-Ag27	35	0	701	32	733
H4-C1-O3-Ag36	44	0	545	0	545
H4-C1-O3-Ag48	56	0	163	0	163
H4-C1-O4-Ag64	73	0	437	0	437
H4-C2-O1-Ag64	71	0	1486	0	1486
H4-C2-O2-Ag27	35	0	19	0	19
H4-C2-O3-Ag20	29	0	5	0	5
H4-C2-O4-Ag11	21	0	12	4	16
H4-C2-O4-Ag12	22	0	526	445	971

H4-C2-O4-Ag24	34	0	46	2	48
H4-C2-O4-Ag26	36	0	5	0	5
H4-C2-O4-Ag27	37	0	400	11	411
H4-C2-O4-Ag64	74	0	10	0	10
H4-C2-O5-Ag24	35	0	12	0	12
H4-C2-O6-Ag44	56	0	318	0	318
H4-C2-O6-Ag60	72	0	59	0	59
H4-C2-O6-Ag74	86	0	20	0	20
H4-C2-O6-Ag76	88	0	127	0	127
H4-C2-O7-Ag41	54	0	101	0	101
H4-C2-O7-Ag43	56	0	106	0	106
H4-C2-O8-Ag45	59	0	100	0	100
H4-C2-O8-Ag64	78	0	28	0	28
H4-C2-O8-Ag76	90	0	30	0	30
H4-C2-O10-Ag41	57	0	99	0	99
H4-C2-O10-Ag43	59	0	90	1	91
H4-C2-O10-Ag45	61	0	108	6	114
H4-C2-O11-Ag42	59	0	176	0	176
H4-C2-O11-Ag43	60	0	487	3	490
H4-C2-O11-Ag44	61	0	96	0	96
H4-C2-O11-Ag45	62	0	183	0	183
H4-C2-O11-Ag53	70	0	7	0	7
H4-C2-O12-Ag20	38	0	36	0	36
H4-C2-O12-Ag41	59	0	299	1	300
H4-C2-O12-Ag42	60	0	112	0	112
H4-C2-O12-Ag43	61	0	207	1	208
H4-C2-O12-Ag44	62	0	98	1	99
H4-C2-O12-Ag53	71	0	124	0	124
H4-C2-O12-Ag77	95	0	20	0	20
H4-C2-O12-Ag78	96	0	20	0	20
H4-C2-O12-Ag85	103	0	46	0	46
H4-C2-O12-Ag86	104	0	20	0	20
H4-C2-O13-Ag41	60	0	97	1	98
H4-C2-O13-Ag45	64	0	277	0	277
H4-C2-O16-Ag116	138	0	619	0	619
H4-C2-O20-Ag92	118	0	101	0	101
H4-C2-O20-Ag93	119	0	40	0	40
H4-C2-O20-Ag95	121	0	89	0	89
H4-C2-O20-Ag96	122	0	89	0	89
H4-C2-O32-Ag56	94	0	80	0	80
H4-C2-O36-Ag211	253	0	9	0	9
H6-C1-O1-Ag27	35	0	62	6	68
H6-C1-O2-Ag27	36	0	413	22	435
H6-C1-O3-Ag12	22	0	132	184	316
H6-C2-O2-Ag36	46	0	530	0	530
H6-C2-O3-Ag36	47	0	523	0	523
H6-C2-O3-Ag48	59	0	161	0	161
H6-C2-O4-Ag36	48	0	517	0	517
H6-C3-O1-Ag48	58	0	160	0	160
H6-C3-O1-Ag64	74	0	1000	0	1000
H8-Ag8	16	9	0	7	16
H8-O6-Ag58	72	0	39	0	39
H8-O12-Ag52	72	0	45	9	54
H8-O16-Ag48	72	0	50	0	50
H8-O22-Ag42	72	0	30	47	77

H8-O30-Ag34	72	0	21	108	129
H8-O36-Ag28	72	0	5	50	55
H8-O40-Ag24	72	0	35	6	41
H8-C1-O2-Ag27	38	0	1	0	1
H8-C2-O2-Ag23	35	0	7	1	8
H8-C2-O2-Ag24	36	0	8	4	12
H8-C3-O2-Ag48	61	0	1056	0	1056
H8-C3-O3-Ag48	62	0	1039	0	1039
H8-C4-O6-Ag75	93	0	20	0	20
H8-C4-O8-Ag96	116	0	20	0	20
H8-C4-O12-Ag87	111	0	20	0	20
H10-O5-Ag12	27	0	109	0	109
H11-Ag5	16	0	0	10	10
H11-O5-Ag12	28	0	54	2	56
H12-O5-Ag12	29	0	43	6	49
H12-C2-O4-Ag12	30	0	380	444	824
H12-C6-O6-Ag76	100	0	30	0	30
H12-C6-O12-Ag88	118	0	30	0	30
H13-O5-Ag12	30	0	40	0	40
H14-O7	21	0	1	808	809
H15-Ag6	21	0	1	0	1
H16-Ag5	21	0	4	0	4
H16-O8	24	0	14	3955	3969
H16-C8-O12-Ag80	116	0	51	0	51
H23-Ag9	32	0	2	0	2
H23-O11-Ag16	50	0	18	325	343
H24-O11-Ag16	51	0	19	167	186
H25-O11-Ag16	52	0	7	127	134
H30-O15	45	124	4	94	222
Total	--	570	19559	27018	47147

1.3 Benchmark of G-NN potential against DFT

To examine the accuracy of G-NN potential for exploring the reaction network of ethene oxidation on pristine Ag(100) and Ag(111) surfaces, we have benchmarked G-NN energetics with DFT results in **Table S2** for 100 randomly selected structures from SSW-RS sampled reaction pairs. The root mean square (RMS) error for the energies of these structures is 2.351 meV/atom, which is low enough to resolve the low energy pathways in the reaction network. In **Table S3**, we also compare the G-NN and DFT result of the calculated barriers in ethene oxidation reaction network, which shows no more than 0.12 eV for the barrier of surface reaction.

Table S2. Benchmark between NN and DFT calculated energies for randomly selected 100 structures in SSW-RS sampled reaction pairs on Ag(100) or Ag(111). Listed data include the species, the number of the species (Num), the maximum (max), minimum (min), and root mean square (RMS) of energy differences (E-diff, in absolute value, meV/atom) between NN and DFT results.

Species	Num	max(E-diff)	min(E-diff)	RMS(E-diff)
Ag(100)				
OxoE*+H*	12	2.727	0.172	1.038
OMC*	9	1.378	0.101	0.808
VA	4	0.756	0.164	0.409
HC≡C*+H_2+OH*	1	9.353	9.353	9.353
HC=C=O*+2H*	10	5.265	1.903	3.884
EO	3	0.467	0.204	0.337
HC=CHOH*+H*	3	4.151	1.057	2.913
HC=CHO*+H_2	6	2.732	0.973	1.829
AA	1	1.442	1.442	1.442
H_2C=CH*+OH*	3	1.892	0.024	1.093
HC≡CH+H_2O	1	3.184	3.184	3.184
H_2C=C*+H_2O	1	2.853	2.853	2.853
CH_2=C=O+2H*	2	8.047	6.226	7.195
Ag(111)				
OxoE*+H*	14	2.550	0.327	1.242
H_2C=C=O+2H*	6	7.433	0.070	3.136
HC=C=O*+H*+H_2	5	2.763	0.415	1.734
CCH_2OH*+H*	6	2.279	0.804	1.533
HC=CHO*+H_2	4	1.829	0.452	1.022
VA	5	2.246	0.257	1.155
AA	2	0.518	0.213	0.396
OMC*	1	0.698	0.698	0.698
$CHCH_2OH$*	1	0.216	0.216	0.216

Total	100	9.353	0.024	2.351

Table S3. Benchmark between NN and DFT calculated energy barriers (E_a) for the surface reactions in ethene oxidation. The surface reactions inlcude: Cyc, OMC* → EO, cyclization; Htr, OMC* → AA, H-transfer; OMC-DH, OMC* → OxoE* + H*, OMC dehydrogenation; Hydro, OxoE* + H* → AA, hydrogenation to form AA; Cyc-Htr, the barrier differences between Cyc and Htr. All the data are in eV.

Reactions	Cyc	Htr	OMC-DH	Hydro
(111)_E_a(DFT)	0.71	0.77	0.78	0.64
(111)_E_a(NN)	0.74	0.84	0.78	0.57
(100)_E_a(DFT)	0.89	0.90	0.58	0.53
(100)_E_a(NN)	0.88	0.84	0.49	0.41

2. Reaction sampling and pathways on Ag(100) surface

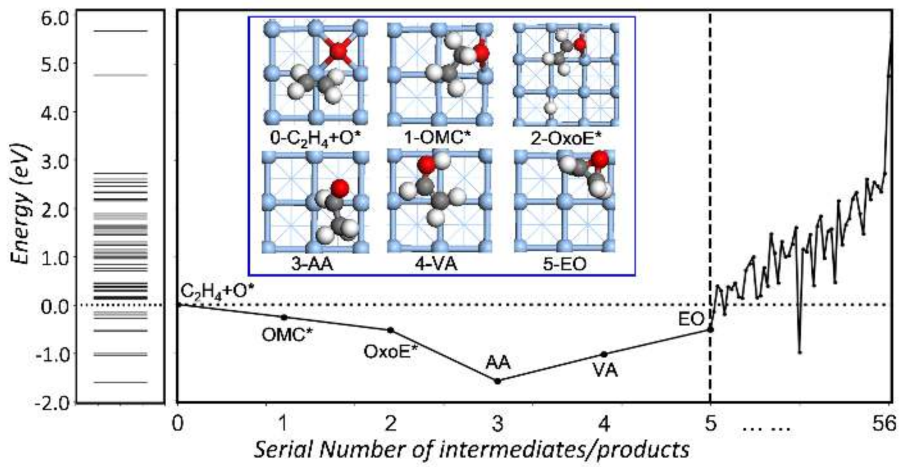

Figure S1. Relative energy of SSW-RS sampled 56 intermediates/products with the reactant defined as an ethene and an atomic adsorbed O on Ag(100). The bar code denotes the energy spectrum, and the figure shows the detailed order of their overall formation barrier from low to high. The names and NN optimized geometries of reactant and structures with overall formation barrier < 1 eV are listed.

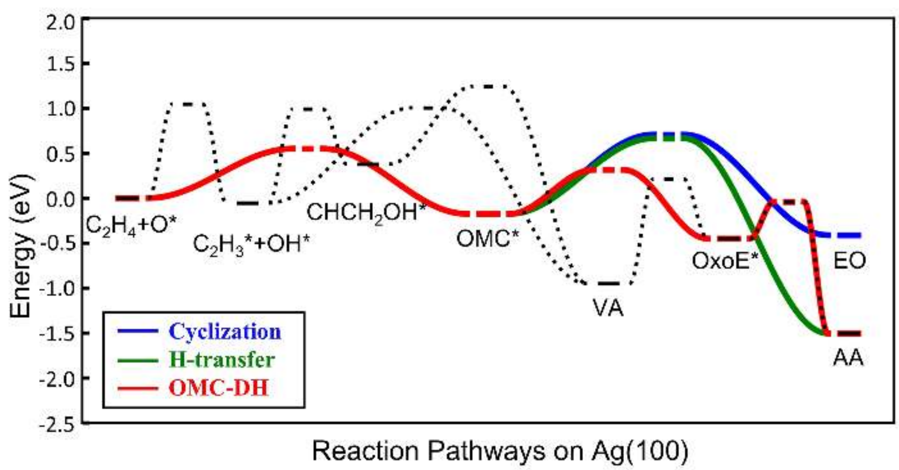

Figure S2. The top 5 pathways with the lowest overall barriers for ethene oxidation on Ag(100) from SSW-RS.

3. More DFT results on pathways

3.1 Comparisons of the ethene oxidation energetics with previous works and different methods

Table S4 shows the barriers computed by different functionals. The order of the barrier remains basically the same in all cases except for the result from RPBE on Ag(111). In particular, all these results confirm the nonselective EO production on Ag(100) with TS2-DH at least 0.22 eV lower than TS2-cyc. This supports our conclusion of the dominant role of OMC-DH pathway on Ag(100). Now we turn to Ag(111), PBE, vdW-PBE, and PW91 support the nonselective EO production, while the RPBE method appears to favor the EO formation with a high selectivity (0.15 eV lower of TS2-cyc than TS2-DH). This is contradictory to all the known experiments, and there is no particular reason for us to believe the RPBE barriers are better than others, since the RPBE functional was originally proposed to reduce the adsorption energy of molecules and was questioned in recent work.[7] We also note that all the previous theoretical work prefers the usage of PBE or PW91 functional to understand ethene epoxidation reaction.

Table S4. Comparisons of the barriers at the TS2 in three different pathways (ZPE corrected) using different DFT XC functionals including RPBE, PW91, and the PBE with vdW correction.

Methods	E_a(Cyc)		E_a(Htr)		E_a(DH)	
	Ag(100)	Ag(111)	Ag(100)	Ag(111)	Ag(100)	Ag(111)
PBE	0.85	0.67	0.78	0.65	0.39	0.57
vdW-PBE	0.91	0.79	0.79	0.65	0.29	0.47
RPBE	0.73	0.52	0.76	0.62	0.51	0.65
PW91	0.86	0.67	0.80	0.67	0.39	0.58

Table S5. The calculated barriers on Ag(111) with different O-coverage.

O-coverage (ML)	1/16	2/16	3/16	4/16
model	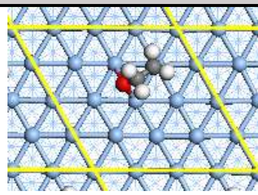	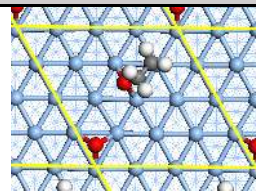	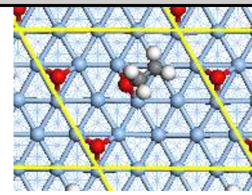	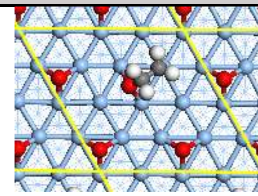
G_a(cyc)	0.67	0.67	0.62	0.59
G_a(Htr)	0.65	0.64	0.58	0.54
G_a(DH)	0.57	0.55	0.56	0.59
ΔG_a(cyc-Htr)	+0.02	+0.03	+0.04	+0.05
ΔG_a(cyc-DH)	+0.10	+0.12	+0.06	+0.00

Table S6. Comparisons of the calculated barriers for ethene epoxidation on Ag(111) and Ag(100). All the data are in eV.

Reactions	G_a(Cyc)	G_a(Htr)	G_a(OMC-DH)	ΔG_a(Cyc-DH)	ΔG_a(Cyc-Htr)
(111) (this work)	0.67	0.65	0.57	+0.10	+0.02
(100) (this work)	0.85	0.78	0.39	+0.46	+0.07
(111) [a]	-	-	-	-	+0.01
(111)[b]	0.73	0.75	-	-	-0.02
(111)[c]	0.79	0.84	-	-	-0.05
(111)[d]	0.74	0.68	-	-	+0.06
(100)[b]	0.92	1.02	-	-	-0.10
(100)[c]	0.75	0.68	-	-	+0.07
(100)[d]	0.51	0.56	-	-	-0.05

[a]: ref.[8] Calculated energies by GGA-PW91 method, on p(3×3) supercell for (111) with a 18 k-points grid, corrected by ZPE and entropies that are obtained from a Ag_{15} cluster model with BP86 method

[b]: ref.[9] Calculated energies by GGA-PW91 method, on p(3×3) supercell for (111) and p(2√2×2√2) supercell for (100) with 3×3×1 Monkhorst-Pack k-mesh

[c]: ref.[10] Calculated energies by GGA-PW91 method, on p(3×3) supercell for (111) and p(2×2) supercell for (100) with 4×4×1 k-mesh, corrected by ZPE

[d]: ref.[11] Calculated energies by GGA-PBE method, on p(4×4) supercell for both (111) and (100) with 2×2×1 k-mesh

3.2 DFT results for the subsequent hydrogenation reactions in OMC-DH pathway

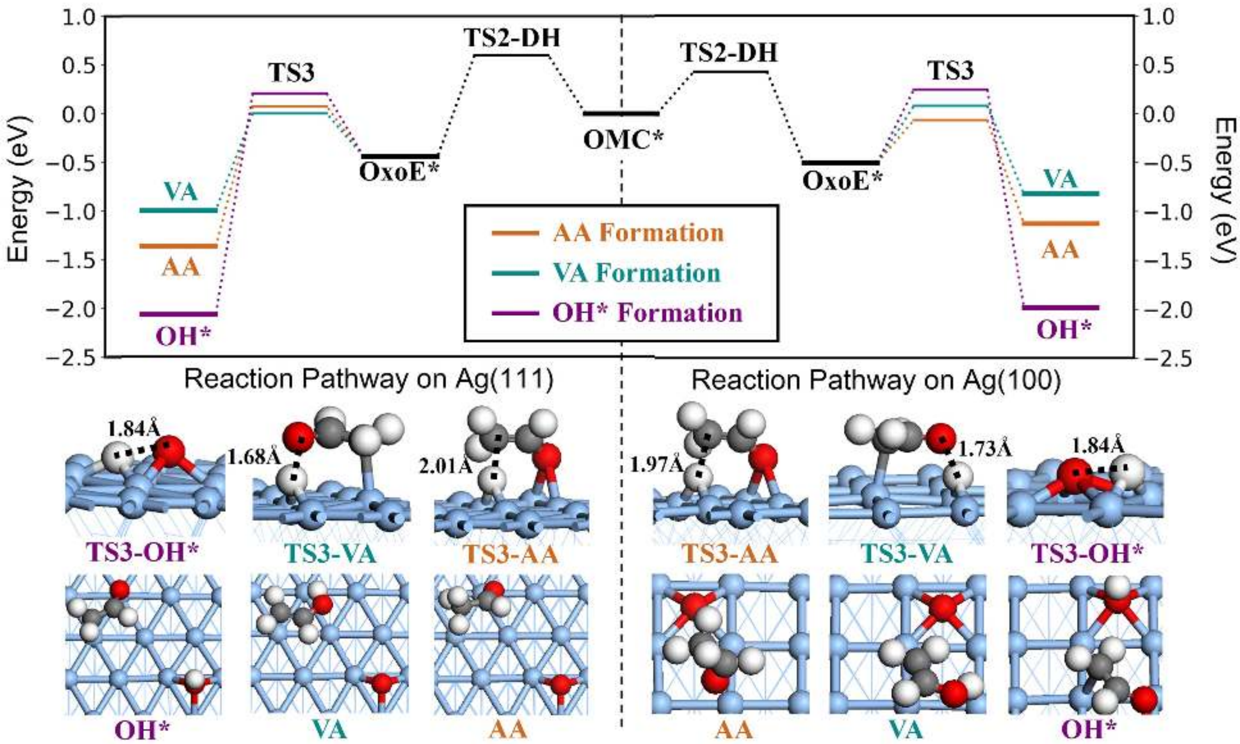

Figure S3. Reaction profiles of the OMC-DH pathway (from OMC to the products) with all the possible subsequent hydrogenation steps considered on Ag(111) and Ag(100). The energies of the corresponding OMC* intermediates on two Ag surfaces are set to be the zero point. Key reaction snapshots are also shown. Ag, blue; C, grey; H, white; O, red.

After the OMC dehydrogenation, the dissociated H atom on surface can take part in three likely hydrogenation reactions. These lead to the formation of various species, including AA, VA, and surface hydroxyl group (OH*), via different TSs, i.e. TS3-AA, TS3-VA, and TS3-OH*, respectively. **Figure S3** shows that In general, Ag(111) and Ag(100) prefer the formation of VA and AA, respectively, while OH* is the thermodynamically favored product but has higher barriers to form on both surfaces. Since VA can convert to AA via the facile keto-enol tautomerism, we, for simplification, use AA formation to represent the subsequent hydrogenation step as shown in **Figure 3**.

4. Microkinetics simulation

A continuous stirred tank model is used in our microkinetics simulation with the contact time being 0.001 s, and the kinetic equations are iteratively solved until the contents of the species are in equilibrium. All the reaction data for microkinetics simulation are shown in Table S7, where the ZPE correction and the entropy correction are included to computed the free energy barrier (G_a). Note that we only compute explicitly the entropy change in the adsorption step of gas phase molecules since the vibrational entropy contribution to adsorbates are generally cancelled[12]. To examine the influence of O_2 pressure, we consider two conditions utilized in experiment, (i) condition I: at the typical industrial conditions with C_2H_4 and O_2 being both at 1 bar, 500 K.54 (ii) condition II: at the low oxygen pressure conditions with 0.63 mbar of ethene and 0.36 mbar of oxygen at 523 K. Only low coverage limits are considered in simulation where the maximum O*(+ O_2*) coverage are set as 0.25 ML and 0.33 ML, respectively[11] (the Ag surface reconstruction occurs at high coverages).

To compare with previous KMC model,[11] we have conducted microkinetics simulations with and without the dehydrogenation pathway. As shown in **Figure S4**, Without the OMC-DH pathway, we found the 0.68/0.66 eV apparent activation energies for EO/AA production, agreeing with the previous kMC model (0.70/0.64 eV). When the OMC-DH pathway is taken into consideration, the apparent activation energies become 0.75/0.66 eV for EO/AA production. This leads to much lower selectivity to EO (~8%), suggesting the presence of OMC-DH will significantly reduce the selectivity. In KMC results, however, it is moderately selective (25-40%) on Ag(111) and highly selective (70-80%) on Ag(100) surfaces. Their selectivity is too high compared with the low pressure experiments on Ag.

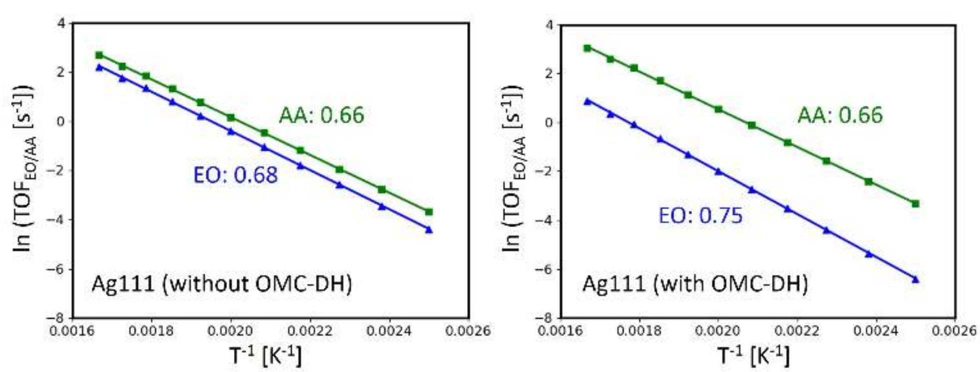

Figure S4. Apparent activation energy plots for microkinetics simulations without (left) and with (right) the OMC-DH pathway on Ag(111). p(C_2H_4) = p(O_2) = 1 bar.

Table S7. The ethene epoxidation reaction energy, ZPE corrections, entropies and Gibbs free energy barriers (forward and reverse, 500 K) for all elementary reactions used in microkinetics simulation. The reaction step can be found in note, where * denotes the surface adsorption site. AA1 and AA2 are the AA from H-transfer and OMC-DH, respectively. The data in Table refers to molecules at 500 K and 1 bar, and the free energy correction due to the pressure in reaction is taken into account in simulation.

Step	Ag(100)							
	$\Delta E_{FS\text{-}IS}$	$\Delta E_{TS\text{-}IS}$	$\Delta ZPE_{FS\text{-}IS}$	$\Delta ZPE_{TS\text{-}IS}$	$T\Delta S_{FS\text{-}IS}$	$T\Delta S_{TS\text{-}IS}$	$G_{a,+}$	$G_{a,-}$
1	-0.64	0.00	0.03	0.00	-0.68	-0.99	0.99	0.92
2	-1.08	0.92	-0.03	-0.04	0.00	0.00	0.88	1.99
3	-0.06	0.00	0.02	0.00	-0.35	-1.06	1.06	0.75
4	-0.27	0.43	0.06	0.01	0.00	0.00	0.44	0.65
5	-0.02	0.89	0.04	-0.04	0.00	0.00	0.85	0.83
6	0.05	0.05	-0.01	-0.01	1.18	0.00	0.04	1.18
7	-1.10	0.90	-0.01	-0.12	0.00	0.00	0.78	1.89
8	0.08	0.08	-0.01	-0.01	1.27	0.00	0.07	1.27
9	-0.33	0.58	-0.21	-0.19	0.00	0.00	0.39	0.93
10	-0.78	0.63	0.20	0.02	0.00	0.00	0.65	1.23
11	0.10	0.10	-0.02	-0.02	1.27	0.00	0.08	1.27

Step	Ag(111)							
	$\Delta E_{FS\text{-}IS}$	$\Delta E_{TS\text{-}IS}$	$\Delta ZPE_{FS\text{-}IS}$	$\Delta ZPE_{TS\text{-}IS}$	$T\Delta S_{TS\text{-}IS}$	$T\Delta S_{TS\text{-}IS}$	$G_{a,+}$	$G_{a,-}$
1	-0.17	0.00	0.01	0.00	-0.52	-0.99	0.99	0.63
2	-0.65	0.96	0.00	-0.03	0.00	0.00	0.93	1.58
3	-0.13	0.00	0.03	0.00	-0.41	-1.06	1.06	0.75
4	-0.37	0.48	0.05	0.00	0.00	0.00	0.48	0.80
5	-0.32	0.71	0.03	-0.04	0.00	0.00	0.67	0.96
6	0.06	0.06	-0.01	-0.01	1.18	0.00	0.05	1.18
7	-1.35	0.77	-0.02	-0.12	0.00	0.00	0.65	2.03
8	0.05	0.05	-0.01	-0.01	1.27	0.00	0.04	1.27
9	-0.32	0.78	-0.16	-0.21	0.00	0.00	0.57	1.05
10	-1.03	0.64	0.13	-0.07	0.00	0.00	0.56	1.46
11	0.04	0.04	-0.01	-0.01	1.27	0.00	0.04	1.27

1	$O_2(g) + * \rightarrow O_2*$
2	$O_2* + * \rightarrow 2\ O*$
3	$C_2H_4(g) + * \rightarrow C_2H_4*$
4	$C_2H_4* + O* \rightarrow OMC* + *$

5	OMC* → EO*
6	EO* → EO(g) + *
7	OMC* → AA1*
8	AA1* → AA1(g) + *
9	OMC* + * → OxoE* + H*
10	OxoE* + H* → AA2* + *
11	AA2* → AA2(g) + *

Table S8. Equilibrium content of chemical species in kinetics simulation at condition I/II for Ag(100)/Ag(111).

Species	C_2H_4(g)	O_2(g)	*	O*	OMC*	OxoE*(H*)	EO(g)	AA1(g)	AA2(g)
100-I	9.87E-1	9.93E-1	6.28E-2	2.57E-2	1.69E-7	2.10E-3	4.77E-6	2.42E-5	1.29E-2
111-I	9.98E-1	9.99E-1	1.00	1.66E-5	7.66E-8	2.66E-4	1.38E-4	2.41E-4	1.48E-3
111-II	3.58E-4	6.29E-4	1.00	4.76E-5	4.93E-11	6.77E-6	1.84E-7	3.13E-7	1.78E-6

Table S9. Microkinetics simulation results at the condition I for Ag(111) using the kinetics data from PBE and PBE-D3 methods, including the selectivity (S%), the conversion (C%), and the content of chemical species at equilibrium.

Method	C_2H_4(g)	O_2(g)	*	O*	OMC*	OxoE*	EO(g)	AA1(g)	AA2(g)	S%	C%
PBE	9.98E-1	9.99E-1	1.00	1.66E-5	7.66E-8	2.66E-4	1.38E-4	2.41E-4	1.48E-3	7.4	0.2
PBE-D3	8.62E-1	9.31E-1	0.74	0.22	9.61E-7	5.13E-3	1.09E-4	2.81E-3	1.35E-1	0.08	13.8

5. Results on the Ag-surf-oxide, Ag_{55}, Cu(111), and Au(111)

Table S10. The Gibbs free energies (G, in eV, 500 K) of all the TSs and intermediates relative to the C_2H_4(g)+O(ads), and the overall free energy barriers ($G_{a,tot}$, in eV) for the six models.

Structures	G(TS1)	G(OMC)	**G(TS2-Cyc)**	**G(TS2-Htr)**	**G(TS2-DH)**	G(OxoE)	G(TS3)	$G_{a,tot}$
Ag(111)	1.45	0.65	**1.32**	**1.30**	**1.22**	0.17	0.73	1.45
Ag(100)	1.46	0.81	**1.66**	**1.59**	**1.20**	0.27	0.82	1.46
Ag-surf-oxide	1.42	1.12	**1.89**	**1.88**	**1.61**	0.44	1.15	1.61
Ag_{55}	1.28	0.65	**1.60**	**1.41**	**1.14**	0.01	0.75	1.28
Cu(111)	1.76	1.11	**2.31**	**2.32**	**1.79**	0.81	1.36	1.79
Au(111)	1.44	0.46	**1.41**	**1.15**	**0.71**	0.15	0.70	1.44

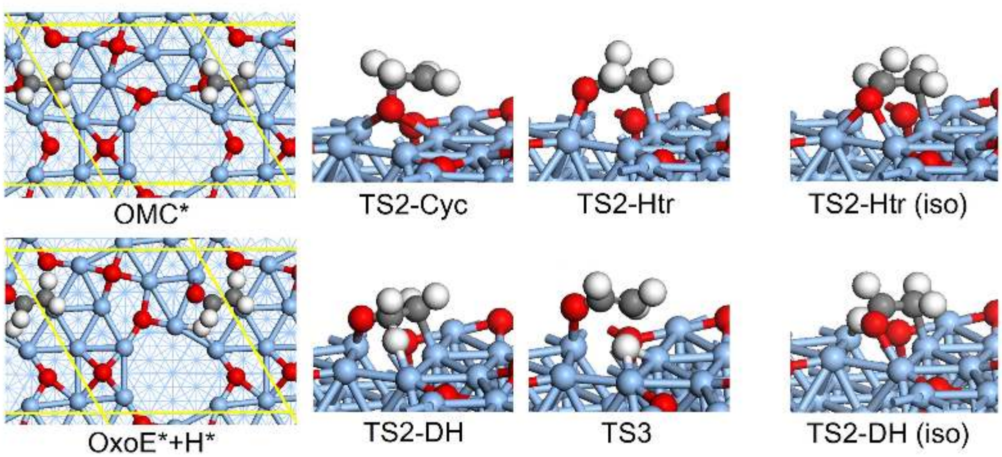

Figure S5. Top view of the OMC and OxoE intermediates, and side view of the three TS2s and TS3 on Ag-surf-oxide. The isomers (iso) of TS2-Htr and TS2-DH are shown in the figure, which are calculated to be energetically indistinguishable with TS2-Htr and TS2-DH, respectively.

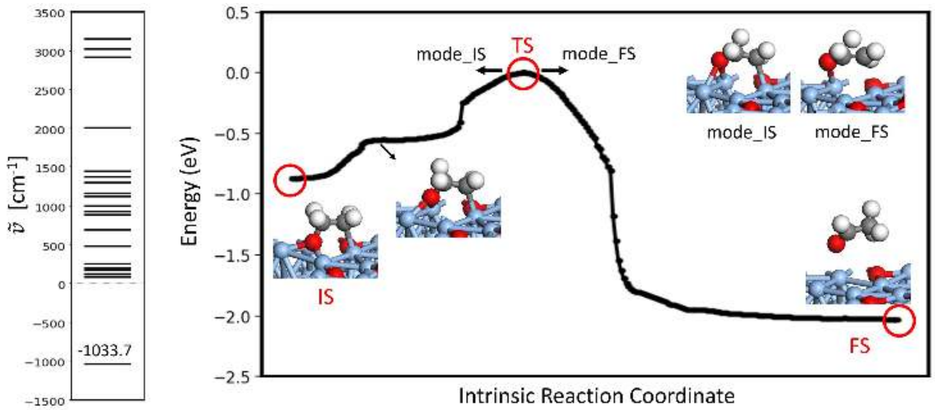

Figure S6. Frequencies and extrapolation optimization results of TS2-Htr on Ag-surf-oxide.

Previous work on Ag-surf-oxide has used a stable TS2-Htr (with a barrier of 0.29 eV) to explain the low selectivity,[13] while we found all the possible TS2-Htr conformations have barriers of 0.76 eV, and the low TS2-DH with barrier of 0.49 eV is the reason for the bad selectivity. The geometries, frequencies and extrapolation optimization results, and XYZ coordinates of our optimized TS2-Htr are shown in Figure S5, S6, and section 6, respectively. Nevertheless, both results confirm the experimental observation of dominant combustion products on Ag-surf-oxide.

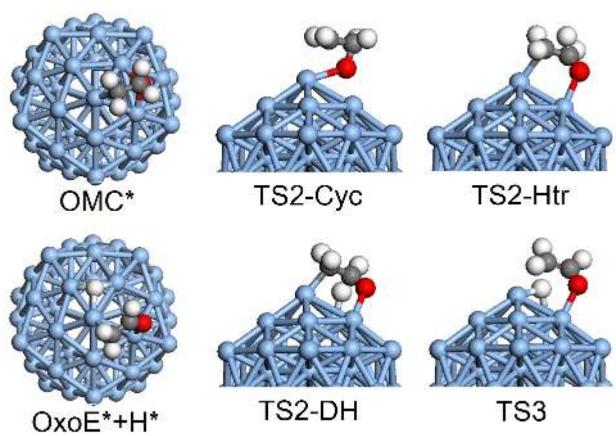

Figure S7. Top view of the OMC and OxoE intermediates, and side view of the three TS2s and TS3 on Ag_{55} cluster.

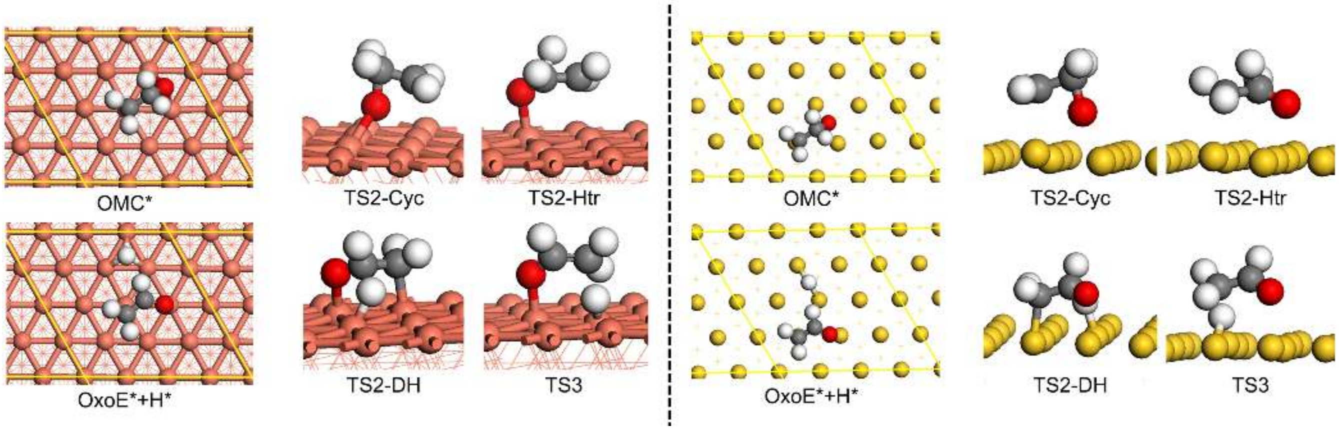

Figure S8. Top view of the OMC and OxoE intermediates, and side view of the three TS2s and TS3 on Cu(111) (left) and Au(111) (right). Color code: C, grey; H, white; O, red; Cu, bronze; Au, yellow.

References

(1) Huang, S.-D.; Shang, C.; Zhang, X.-J.; Liu, Z.-P. Material Discovery by Combining Stochastic Surface Walking Global Optimization with a Neural Network. *Chem. Sci.* **2017**, *8*, 6327-6337.

(2) Huang, S.-D.; Shang, C.; Kang, P.-L.; Liu, Z.-P. Atomic Structure of Boron Resolved Using Machine Learning and Global Sampling. *Chem. Sci.* **2018**, *9*, 8644-8655.

(3) Shang, C.; Huang, S.-D.; Liu, Z.-P. Massively Parallelization Strategy for Material Simulation Using High-Dimensional Neural Network Potential. *J. Comput. Chem.* **2019**, *40*, 1091-1096.

(4) Shang, C.; Liu, Z.-P. Stochastic Surface Walking Method for Structure Prediction and Pathway Searching. *J. Chem. Theory Comput.* **2013**, *9*, 1838-1845.

(5) Zhang, X.-J.; Shang, C.; Liu, Z.-P. From Atoms to Fullerene: Stochastic Surface Walking Solution for Automated Structure Prediction of Complex Material. *J. Chem. Theory Comput.* **2013**, *9*, 3252-3260.

(6) Shang, C.; Zhang, X.-J.; Liu, Z.-P. Stochastic Surface Walking Method for Crystal Structure and Phase Transition Pathway Prediction. *Phys. Chem. Chem. Phys.* **2014**, *16*, 17845-17856.

(7) Wellendorff, J.; Silbaugh, T. L.; Garcia-Pintos, D.; Nørskov, J. K.; Bligaard, T.; Studt, F.; Campbell, C. T. A Benchmark Database for Adsorption Bond Energies to Transition Metal Surfaces and Comparison to Selected DFT Functionals. *Surf. Sci.* **2015**, *640*, 36–44.

(8) Linic, S.; Barteau, M. A. Control of Ethylene Epoxidation Selectivity by Surface Oxametallacycles. *J. Am. Chem. Soc.* **2003**, *125*, 4034–4035.

(9) Christopher, P.; Linic, S. Engineering Selectivity in Heterogeneous Catalysis: Ag Nanowires as Selective Ethylene Epoxidation Catalysts. *J. Am. Chem. Soc.* **2008**, *130*, 11264–11265.

(10) Ozbek, M. O.; Onal, I.; van Santen, R. A. Effect of Surface and Oxygen Coverage on Ethylene Epoxidation. *Top. Catal.* **2012**, *55*, 710–717.

(11) Hus, M.; Hellman, A. Ethylene Epoxidation on Ag(100), Ag(110), and Ag(111): A Joint Ab Initio and Kinetic Monte Carlo Study and Comparison with Experiments. *ACS Catal.* **2019**, *9*, 1183–1196.

(12) Hong, Q.-J.; Liu, Z.-P. Mechanism of CO2 Hydrogenation over Cu/ZrO2((2)over-Bar12) Interface from First-Principles Kinetics Monte Carlo Simulations. *Surf. Sci.* **2010**, *604*, 1869–1876.

(13) Jones, T. E.; Wyrwich, R.; Boecklein, S.; Rocha, T. C. R.; Carbonio, E. A.; Knop-Gericke, A.; Schloegl, R.; Guenther, S.; Wintterlin, J.; Piccinin, S. Oxidation of Ethylene on Oxygen Reconstructed Silver Surfaces. *J. Phys. Chem. C* **2016**, *120*, 28630–28638.

6. XYZ coordinates for important structures along OMC-DH pathway

Here, TS2-DH and TS3 on Ag(100) and Ag(111), and TS2-Htr and TS2-DH on Ag-surf-oxide are provided in VASP POSCAR format.

```
# TS2-DH of Ag(100)
1.000000000000
    11.72930000     0.00000000     0.00000000
     0.00000002    11.72930000     0.00000000
     0.00000004     0.00000004    21.00000000
    H     C     O    Ag
    4     2     1    64
Cart
   5.58022150     5.49424958    14.08099023
   7.00293824     6.55883691    13.61493830
   6.68603420     3.32541031    12.62988901
   7.21576284     3.71801399    14.32559938
   6.49052248     5.59796425    13.48307611
   7.39697187     4.46868577    13.53073185
   8.61696450     4.53625028    13.06989159
   7.32473026     1.46304731     5.04919202
  10.25948730     1.46124308     5.04981979
   1.46202183     4.39292568     5.04960932
   4.39430511     4.39430532     5.04906954
   7.32610817     4.39270385     5.05121983
  10.25895697     4.39275659     5.05019571
   1.46182403     1.46182440     5.05208080
   1.46304710     7.32473057     5.04919192
   4.39270333     7.32610801     5.05121904
   7.32565047     7.32565086     5.05186099
```

10.25800410	7.32486402	5.05162294
1.46124268	10.25948748	5.04981941
4.39275601	10.25895693	5.05019613
7.32486379	10.25800441	5.05162327
10.25749809	10.25749818	5.05136351
4.39292515	1.46202190	5.04960925
5.86467000	11.72929987	7.08570000
8.79700500	11.72929987	7.08570000
-0.00000000	11.72929987	7.08570000
0.00000000	2.93233487	7.08570000
2.93233500	2.93233487	7.08570000
5.86467000	2.93233487	7.08570000
8.79700500	2.93233487	7.08570000
0.00000000	5.86466987	7.08570000
2.93233500	5.86466987	7.08570000
5.86467000	5.86466987	7.08570000
8.79700500	5.86466987	7.08570000
0.00000000	8.79700487	7.08570000
2.93233500	8.79700487	7.08570000
5.86467000	8.79700487	7.08570000
2.93233500	11.72929987	7.08570000
8.79700500	8.79700487	7.08570000
4.39791053	1.47066584	9.13716304
7.33329720	1.48666714	9.15411809
10.24557434	1.48379220	9.16536911
1.46042310	4.39562699	9.12677553
4.43898789	4.39859474	9.17259812
7.32905155	4.40256543	9.18959496
10.22304421	4.39564809	9.17895497
1.46845605	7.33897669	9.12918004
4.42476083	7.29555088	9.16285441
1.45375579	1.45486053	9.13541534
7.32851009	7.27728914	9.18963440
10.24563954	7.31263241	9.15727553
1.46475172	10.26766325	9.14905989
4.39480467	10.25154475	9.14189353
7.32644574	10.25207544	9.12988983
10.26983400	10.26636922	9.12912750
5.86364625	11.67627477	11.17077742
8.79802902	11.69902812	11.16382893
0.00833548	2.92651562	11.16824055
2.89174610	2.92720748	11.15178964
11.72915917	11.72434227	11.18034299
5.78341617	2.81796430	11.21914338
8.80574293	2.85850560	11.25406857
0.05003086	5.87197322	11.16041157
2.90755789	5.85801834	11.15818227
5.79629479	5.88622277	11.34414881
8.88221148	5.95115065	11.25758742
11.72368321	8.79722147	11.16457412
2.92872242	8.79360737	11.16559504
5.86279897	8.80120584	11.17778026
8.79944416	8.83395343	11.15967268
2.93810929	11.72901822	11.17037205

TS3 of Ag(100)
1.000000000000

11.72930000	0.00000000	0.00000000
0.00000002	11.72930000	0.00000000
0.00000004	0.00000004	21.00000000

H	C	O	Ag
4	2	1	64

Cart

5.96792544	4.50777216	12.41398150
6.84650941	6.35028787	13.54477296
5.96170094	5.21502769	14.73124083
7.75465378	3.55640718	14.55602542
6.75360167	5.35665988	13.99612098
7.80578930	4.46105348	13.92184944
8.80556039	4.52669565	13.09861249
7.32473026	1.46304731	5.04919202
10.25948730	1.46124308	5.04981979
1.46202183	4.39292568	5.04960932
4.39430511	4.39430532	5.04906954
7.32610817	4.39270385	5.05121983
10.25895697	4.39275659	5.05019571
1.46182403	1.46182440	5.05208080
1.46304710	7.32473057	5.04919192
4.39270333	7.32610801	5.05121904
7.32565047	7.32565086	5.05186099
10.25800410	7.32486402	5.05162294
1.46124268	10.25948748	5.04981941
4.39275601	10.25895693	5.05019613
7.32486379	10.25800441	5.05162327
10.25749809	10.25749818	5.05136351
4.39292515	1.46202190	5.04960925
5.86467000	11.72929987	7.08570000
8.79700500	11.72929987	7.08570000
-0.00000000	11.72929987	7.08570000
0.00000000	2.93233487	7.08570000
2.93233500	2.93233487	7.08570000
5.86467000	2.93233487	7.08570000
8.79700500	2.93233487	7.08570000
0.00000000	5.86466987	7.08570000
2.93233500	5.86466987	7.08570000
5.86467000	5.86466987	7.08570000
8.79700500	5.86466987	7.08570000
0.00000000	8.79700487	7.08570000
2.93233500	8.79700487	7.08570000
5.86467000	8.79700487	7.08570000
2.93233500	11.72929987	7.08570000
8.79700500	8.79700487	7.08570000
10.27109127	10.27217993	9.14145437
7.32687425	10.28566431	9.13868181
1.45891768	4.39443886	9.13656741
1.46705534	7.34274429	9.13609573
1.47058204	1.45493578	9.14180901
4.41001640	1.47849360	9.16463891
4.39327272	10.27848231	9.14394629

1.46778440	10.26407033	9.15802751
4.38889413	4.40344594	9.12328704
10.24695279	4.40204828	9.16420213
7.32382452	1.51088523	9.19284885
10.24401326	7.32399793	9.15899560
4.40626821	7.34007221	9.15467465
10.24295942	1.48516388	9.16305491
7.32856596	7.32147725	9.17824784
7.35045760	4.41324279	9.16766323
8.79305154	8.84683616	11.16984419
0.01890978	2.92257910	11.16788489
0.03026901	5.87264001	11.16059220
2.90379440	2.92718715	11.17446531
-0.00209394	11.72736806	11.18251930
8.79307331	-0.00020203	11.18214116
-0.00211207	8.79899400	11.17969700
2.89901223	5.87122464	11.16625507
5.80361833	3.00434761	11.24739592
2.93745992	11.72654069	11.18973045
2.93722530	8.80180946	11.18616970
5.86254336	0.03596568	11.18677679
5.86126909	8.82826087	11.16636273
8.81735520	2.89963139	11.25299248
8.83734976	5.95728707	11.24578302
5.79566888	5.88071971	11.19689492

TS2-DH of Ag(111)
1.000000000000

11.72940000	0.00000000	0.00000000
-5.86469998	10.15795839	0.00000000
0.00000004	0.00000007	22.00000000

H	C	O	Ag
4	2	1	64

Cart

5.18917985	7.41611708	14.57313324
3.91103833	8.69614423	14.37800967
3.66579201	5.50971578	13.45145732
3.33458692	6.01933211	15.21768555
4.22861294	7.67910625	14.11625723
3.15598822	6.68667134	14.34234569
1.91575333	6.93047702	14.06925301
2.90187257	5.01263788	4.71383470
-0.02218215	5.00219195	4.71764695
1.44198437	7.55048715	4.71898983
-1.48275837	7.54135586	4.71570830
1.44002856	2.46468268	4.71548172
5.83546762	5.01140010	4.70917893
4.37275938	7.54860448	4.71588519
4.36717292	2.47353050	4.71302100
7.29722122	2.47247767	4.70983126
-2.94938264	10.08223365	4.71715804
7.31639039	7.53682155	4.71702346
8.77635683	4.99999039	4.71851968
-0.02521283	10.09159933	4.71753229

10.23882764	2.46185467	4.71803248
2.90514081	10.08922934	4.71727428
5.84741330	10.07810717	4.72752206
-0.00695794	1.59101267	7.12530543
-0.00388478	6.66301677	7.12922101
-1.47346105	4.13045067	7.12755502
1.45454249	4.12875748	7.12946734
-1.46302252	9.19993454	7.12286616
1.46069142	9.20756127	7.12294715
2.92251774	1.58890786	7.12724221
-2.93221929	6.66010493	7.12111233
2.92168731	6.66975867	7.12784007
4.38289601	4.13552123	7.12090887
-4.39260938	9.20273488	7.12085204
4.38833134	9.20495968	7.12269918
5.84894076	1.59377116	7.12149703
5.85308753	6.66899338	7.11923306
7.31243174	4.13372865	7.11843336
8.77452846	1.59772830	7.11689741
10.25786141	0.74195472	9.46368438
5.85452459	8.35701039	9.47135148
1.46564486	0.73674995	9.46892578
7.32935960	0.73925928	9.46851418
8.78925051	3.28704122	9.46909997
4.39761761	0.74144796	9.46337272
7.31311122	5.82076407	9.48757345
2.93250863	3.29332750	9.48181481
4.39557444	5.84592015	9.51433354
5.85241222	3.29026604	9.48040294
2.93471724	8.34236919	9.52037787
-0.00102710	3.28644617	9.47428882
-2.92751320	8.35885946	9.46179736
-1.46602214	5.81881300	9.48085125
0.02517731	8.34363448	9.50613857
1.49162215	5.82420918	9.54005337
-0.00883466	10.06627264	11.83618882
5.88686413	10.09567166	11.83153550
10.25524541	2.44620941	11.83866674
8.78674765	4.97148211	11.84889406
2.92962704	10.08898558	11.82308011
7.36701408	7.51584212	11.82831336
-2.92860423	10.04964531	11.83834626
1.45801186	2.42221686	11.83849080
7.33286471	2.43565150	11.84554275
4.49572692	7.61258279	11.90842276
2.99254618	4.87070781	11.88334204
4.41318113	2.39021116	11.84691463
5.87631070	4.95548795	11.88122192
-1.48450549	7.51204591	11.83754745
1.42760391	7.54764139	11.92755398
-0.01590792	4.95532654	11.84121278

TS3 of Ag(111)
1.000000000000

11.72940000	0.00000000	0.00000000
-5.86469998	10.15795839	0.00000000
0.00000004	0.00000007	22.00000000
H	C	O	Ag
4	2	1	64

Cart

4.69183984	6.61798085	15.56992976
4.91337206	8.14373091	14.52020868
4.57542496	6.22575792	13.17215295
2.27286722	6.66162984	15.22838791
4.26912117	7.33150291	14.86203894
2.89173391	7.42428762	14.71456300
2.26644344	8.27430761	13.96555133
2.90187257	5.01263788	4.71383470
-0.02218215	5.00219195	4.71764695
1.44198437	7.55048715	4.71898983
-1.48275837	7.54135586	4.71570830
1.44002856	2.46468268	4.71548172
5.83546762	5.01140010	4.70917893
4.37275938	7.54860448	4.71588519
4.36717292	2.47353050	4.71302100
7.29722122	2.47247767	4.70983126
-2.94938264	10.08223365	4.71715804
7.31639039	7.53682155	4.71702346
8.77635683	4.99999039	4.71851968
-0.02521283	10.09159933	4.71753229
10.23882764	2.46185467	4.71803248
2.90514081	10.08922934	4.71727428
5.84741330	10.07810717	4.72752206
-0.00695794	1.59101267	7.12530543
-0.00388478	6.66301677	7.12922101
-1.47346105	4.13045067	7.12755502
1.45454249	4.12875748	7.12946734
-1.46302252	9.19993454	7.12286616
1.46069142	9.20756127	7.12294715
2.92251774	1.58890786	7.12724221
-2.93221929	6.66010493	7.12111233
2.92168731	6.66975867	7.12784007
4.38289601	4.13552123	7.12090887
-4.39260938	9.20273488	7.12085204
4.38833134	9.20495968	7.12269918
5.84894076	1.59377116	7.12149703
5.85308753	6.66899338	7.11923306
7.31243174	4.13372865	7.11843336
8.77452846	1.59772830	7.11689741
10.24138664	0.74507617	9.49108211
5.86304214	8.37456383	9.46916319
1.46621567	0.75639650	9.46755936
7.33233459	0.74245794	9.49904185
8.78561426	3.29045252	9.47811157
4.39913010	0.75633831	9.46727637
7.31206619	5.82396031	9.49726394
2.92950921	3.29375404	9.48514066
4.39607421	5.82641679	9.46138647
5.85716759	3.31044247	9.50826505

2.92835035 8.36339980 9.52322537
-0.01296499 3.28789954 9.48161757
-2.92973101 8.36913405 9.46242094
-1.47520355 5.82795983 9.48219899
0.01061935 8.36264444 9.49890062
1.46697345 5.84212969 9.51763546
-0.02378093 10.09378772 11.83843694
5.87691802 10.09046909 11.82511414
10.25256538 2.44771550 11.85785812
8.77824401 4.98353117 11.85044916
2.94496014 10.06683355 11.91123060
7.37594366 7.55074635 11.83215101
-2.93459407 10.08172142 11.84197593
1.46454170 2.46180929 11.84463013
7.31793127 2.46552180 11.85802722
4.46685620 7.51479874 11.82150106
2.94578067 4.98658725 11.86677074
4.39331296 2.44642652 11.85695140
5.82868462 5.02488566 11.98347120
-1.48182330 7.52506937 11.85013794
1.40928899 7.52805090 11.90853610
-0.01590838 4.97530314 11.85156328

TS2-Htr of Ag-surf-oxide
1.000000000000
11.72940000 0.00000000 0.00000000
-5.86469998 10.15795839 0.00000000
0.00000004 0.00000007 22.00000000
H C O Ag
4 2 6 76
Cart
-2.83443388 6.31636707 17.15194140
6.61678495 5.46138403 17.25328239
7.16490321 7.14582345 17.75836517
-3.38741513 7.91100127 16.32618456
-3.59891321 6.87031118 16.60116684
6.73877625 6.46736982 16.80612535
-3.38544069 9.27012666 14.15246946
8.30294842 2.30787616 14.11305279
2.48696712 5.77166765 14.11369908
0.70525554 8.72102044 14.88238339
5.70917875 6.99256952 16.20673591
0.01565386 2.44412314 14.84192030
5.83546762 5.01140010 4.70917893
7.29722122 2.47247767 4.70983126
4.36717292 2.47353050 4.71302100
2.90187257 5.01263788 4.71383470
1.44002856 2.46468268 4.71548172
-1.48275837 7.54135586 4.71570830
4.37275938 7.54860448 4.71588519
7.31639039 7.53682155 4.71702346
-2.94938264 10.08223365 4.71715804
2.90514081 10.08922934 4.71727428
-0.02521283 10.09159933 4.71753229

-0.02218215	5.00219195	4.71764695
10.23882764	2.46185467	4.71803248
8.77635683	4.99999039	4.71851968
1.44198437	7.55048715	4.71898983
5.84741330	10.07810717	4.72752206
8.77452846	1.59772830	7.11689741
7.31243174	4.13372865	7.11843336
5.85308753	6.66899338	7.11923306
-4.39260938	9.20273488	7.12085204
4.38289601	4.13552123	7.12090887
-2.93221929	6.66010493	7.12111233
5.84894076	1.59377116	7.12149703
4.38833134	9.20495968	7.12269918
-1.46302252	9.19993454	7.12286616
1.46069142	9.20756127	7.12294715
-0.00695794	1.59101267	7.12530543
2.92251774	1.58890786	7.12724221
-1.47346105	4.13045067	7.12755502
2.92168731	6.66975867	7.12784007
-0.00388478	6.66301677	7.12922101
1.45454249	4.12875748	7.12946734
1.46589303	5.78999800	9.49831621
4.38438218	5.81416554	9.49143707
4.37201108	0.72316372	9.52519720
5.87129155	8.35085423	9.47927066
7.33199601	0.72846353	9.50622324
-0.00953745	8.35455629	9.48269975
2.93703512	8.34299446	9.47212993
10.25669072	0.72232076	9.47162952
7.32987357	5.81667786	9.46735542
2.93659494	3.28832519	9.52623676
0.00534274	3.26504643	9.48743705
1.46545031	0.72675806	9.51774838
-1.46305583	5.81257570	9.48299070
8.77873789	3.27520618	9.48571034
-2.93572811	8.35319155	9.51928603
10.26280542	2.39613196	11.78952772
5.85248767	4.93712308	11.79912146
2.93802361	4.95768054	11.94139890
7.33263160	2.37334667	11.90951766
1.48490481	2.41541502	11.88740029
7.31193545	7.46224703	11.86961191
-2.93364084	10.03159286	11.93950784
8.80051102	4.97069876	11.83440720
1.46025895	7.48762929	11.78608798
4.43917585	7.50147099	11.86398942
5.85200362	10.03865774	11.87778814
-0.01991999	4.92120542	11.85637405
-2.90481157	6.59957098	14.23738031
-1.54952498	4.05868738	14.22362530
10.17869715	0.72350199	14.20782680
5.87454616	8.42593054	14.26401241
2.94179692	8.19244953	14.19940557
0.05417065	6.56933073	14.20354427
-1.29430587	9.13738279	14.40727038

7.28700532	0.48464274	14.42101584
1.35409441	0.88104102	14.42285540
7.20451986	4.25222029	14.15096412
4.75782361	5.73773783	14.25291673
1.35843061	4.01403949	14.42104587

TS2-DH of Ag-surf-oxide

1.000000000000

11.72940000	0.00000000	0.00000000
-5.86469998	10.15795839	0.00000000
0.00000004	0.00000007	22.00000000

H	C	O	Ag
4	2	6	76

Cart

-2.83394901	6.55563565	17.08294988
6.84746057	5.37157080	15.59790467
6.64890942	5.74034850	17.30387593
-3.57749217	8.08312063	16.37105101
-3.57065291	6.98778177	16.39713305
6.81861772	6.37607777	16.40424762
-3.44418712	9.42698254	14.00548380
8.29151765	2.20838897	14.02753219
2.43127720	5.82276918	14.08062582
0.60458111	8.71887151	14.91945886
5.74824447	7.11444717	16.06554895
0.01085062	2.50491774	14.97468956
5.83546762	5.01140010	4.70917893
7.29722122	2.47247767	4.70983126
4.36717292	2.47353050	4.71302100
2.90187257	5.01263788	4.71383470
1.44002856	2.46468268	4.71548172
-1.48275837	7.54135586	4.71570830
4.37275938	7.54860448	4.71588519
7.31639039	7.53682155	4.71702346
-2.94938264	10.08223365	4.71715804
2.90514081	10.08922934	4.71727428
-0.02521283	10.09159933	4.71753229
-0.02218215	5.00219195	4.71764695
10.23882764	2.46185467	4.71803248
8.77635683	4.99999039	4.71851968
1.44198437	7.55048715	4.71898983
5.84741330	10.07810717	4.72752206
8.77452846	1.59772830	7.11689741
7.31243174	4.13372865	7.11843336
5.85308753	6.66899338	7.11923306
-4.39260938	9.20273488	7.12085204
4.38289601	4.13552123	7.12090887
-2.93221929	6.66010493	7.12111233
5.84894076	1.59377116	7.12149703
4.38833134	9.20495968	7.12269918
-1.46302252	9.19993454	7.12286616
1.46069142	9.20756127	7.12294715
-0.00695794	1.59101267	7.12530543
2.92251774	1.58890786	7.12724221

-1.47346105	4.13045067	7.12755502
2.92168731	6.66975867	7.12784007
-0.00388478	6.66301677	7.12922101
1.45454249	4.12875748	7.12946734
1.46617966	5.78988347	9.49743318
4.39116111	5.81220447	9.50736512
4.37969211	0.72909940	9.51497747
5.87544014	8.34897404	9.49261922
7.32989366	0.72431133	9.49496191
-0.01511388	8.34994893	9.48691761
2.93859123	8.33483535	9.47705715
10.25443690	0.71753180	9.46699807
7.33007864	5.82125105	9.49362957
2.93469544	3.28912819	9.52338068
0.00205381	3.26872954	9.48424885
1.45905554	0.73207349	9.50686897
-1.47372004	5.81010103	9.49203145
8.77728450	3.28875925	9.48399447
-2.93950358	8.35307434	9.51461976
5.87561849	3.25990426	9.49100008
2.92834949	9.96596914	11.85485643
-1.46745761	7.48806737	11.87962704
-0.01557534	10.03652350	11.87577571
4.41005962	2.43786297	11.88495296
10.25636449	2.39902141	11.77066225
5.88490170	4.93397565	11.84437225
2.94064128	4.95613560	11.93821653
7.32594474	2.37404342	11.86670033
1.47690321	2.43587855	11.88367933
7.33382999	7.48467010	11.92452963
-2.92881024	10.06960227	11.88403464
8.77958182	4.97818390	11.89521400
1.45581595	7.48495718	11.78969537
4.45745628	7.49332233	11.88458500
5.84421904	10.04729166	11.88185678
-0.02804681	4.92902297	11.85788444
-2.79595219	6.57212132	14.32706396
-1.53329274	4.01237120	14.18904813
10.16058290	0.74582458	14.19820156
5.84433311	8.47163352	14.28219794
2.92244008	8.19535207	14.20814298
0.05435844	6.59728278	14.19980732
-1.37343849	9.19488341	14.38219155
7.23810973	0.42688883	14.41031218
1.30046937	0.98008007	14.40507711
7.12419014	4.06686197	14.26894505
4.69270685	5.67278475	14.26168190
1.35110679	4.04851079	14.45831964